

Regularized GAN-Augmented CNNs for Enhanced Rheumatoid Arthritis Detection

Saloni Fathima *¹, G. Shankar Lingam²

Submitted: 28/01/2024 Revised: 06/03/2024 Accepted: 14/03/2024

Abstract: Rheumatoid arthritis (RA), a chronic joint disease with significant implications for patient health, demands early detection and management to mitigate its potentially severe consequences. The advancement of artificial intelligence, the computer-based automatic diagnosing systems has significantly reduced human involvement in diagnosing the disease. Numerous research endeavors have focused on leveraging machine learning (ML) and deep learning (DL) algorithms to automate RA detection methods. These studies concentrate on various joints affected by RA, such as the hands, knees, and feet, providing a rapid and precise means of identification. Early detection facilitated by these advanced technologies is key to effective intervention and improved patient outcomes. This paper presents the enhanced deep learning model that can automatically detect RA. In this, we used a Kaggle knee x-ray data set; due to the less number of samples, we first augmented the samples with regularized GAN and balanced the images. Finally, these samples are trained on an optimized neural network model. In this, we got an accuracy of 0.97. Moreover, we tested all dimensions to prove the consistency of the model, and our model consistently performed with other prescribed models.

Key words. Rheumatoid arthritis, knee images, R-GAN, deep learning, CNN

1. Introduction

RA is a chronic bone disease that predominantly affects the joints within the body. Despite the absence of a cure for RA, effective management strategies have been established. Early detection and intervention are crucial, as neglecting the condition's initial stages can lead to severe, life-altering consequences. The progression of RA unfolds through four stages, culminating in bony ankylosis, which inflicts significant damage on the body. Presently, RA diagnosis involves various methods such as MRI imaging, blood samples, and nerve condition techniques, with medical imaging, particularly MRI, being the prevalent diagnostic tool.

Incorporating artificial intelligence (AI) and ML into healthcare has substantially reduced human involvement in the diagnostic process. Computer-based automatic diagnosing systems have emerged as practical tools for identifying and accurately assessing RA. Extensive research efforts have been dedicated to refining RA detection methods, focusing on joints like the hands, knees, and head.

The application of AI and ML in healthcare holds promise for advancing RA diagnostics and providing efficient and accurate automated systems that contribute to timely interventions and improved patient outcomes.

The pursuit of refining RA detection methods has driven extensive research, especially in joints where RA primarily manifests, such as the hands, knees, and head. Previous studies, like Snehalatha U in [1, 2, 4, and 5], worked on knee and joint regions and have explored numerous algorithms and extracted diverse features from thermal images to enhance diagnostic precision, implementing machine learning models. However, challenges have surfaced in [5] as the field advances, highlighting the need for more samples for training deep learning models.

Beyond detection nuances, the exploration of RA extends to classification and segmentation. Researchers have delved into various anatomical regions, including the hands, knees, and head. Each region presents unique challenges and considerations, requiring the application of diverse algorithms and methodologies, as demonstrated in the comprehensive body of work, like the neck and hand regions of the body encapsulated in [1, 2, 3, 13, and 14]. Furthermore, the interdisciplinary nature of healthcare research is evident in endeavors such as [12,17,18], where researchers have investigated the correlation between RA and cardiovascular disease (CVD). Understanding the risk levels associated with RA on CVD interconnectedness of various health domains.

1.1. Contributions

1. Developed a Regularized Generative Adversarial Network (GAN) to generate synthetic samples.
2. Trained a finely-tuned Convolutional Neural Network (CNN) model using a combination of authentic and synthetic samples.
3. Presented superior performance of the proposed model compared to existing models in the field.

2. Related Work

The landscape of rheumatoid arthritis (RA) research is vast and

1 Research Scholar, Department of Computer Science and Engineering, Chaitanya Deemed to be University, Warangal, Telangana – 506001, India.

ORCID ID: 0009-0001-3373-9245

2 Department of Computer Science and Engineering, Chaitanya Deemed to be University, Warangal, Telangana – 506001, India.

ORCID ID: 0009-0005-6809-6728

ORCID ID : 0000-3343-7165-777X

** Corresponding Author Email: author@email.com*

diverse, with numerous studies employing various imaging and machine learning techniques to enhance the disease's detection, diagnosis, and understanding.

Snehalatha et al. [1, 2, 3] Utilized supervised and unsupervised machine learning models for automated X-ray and thermal imaging analysis. Implemented algorithms like the fast greedy snake algorithm and k-means clustering for knee and hand region RA assessment. They Explored ultrasound image segmentation and feature extraction in MCP and wrist regions for RA evaluation.

Bardhan & Bhowmik [6] Proposed a two-stage classification model for knee joint thermograms using the seeded region growing method and support vector machine. They have achieved an accuracy of 0.91 in classifying arthritis, highlighting the potential of these techniques in predicting subclinical inflammation.

Ahalya et al. [8] Developed a customized neural network model (RA Net) for RA detection in hand thermal images. Employed a convolutional neural network to classify healthy and unhealthy regions, achieving high accuracies of 0.95 and 0.97, respectively. Srinivasan et al. [9] Combined CRNN and VGG16-enhanced Region Proposal Network for knee RA detection and grade classification. A notable accuracy of 0.97 was achieved by training the model with 3192 X-ray samples, showcasing the effectiveness of this hybrid approach.

Xiao et al. [10] Investigated machine learning models and emphasized the importance of feature extraction in AI models. Employed weighted gene co-expression network analysis (WGCNA) and differentially expressed genes for training ML models, demonstrating the significance of extracted features in model performance.

Chen et al. [11] Utilized machine learning to identify immune-related biomarkers of RA based on weighted gene co-expression network analysis (WGCNA). Trained ML models like SVM and achieved an accuracy of 0.85, classifying different cells involved in the disease.

Khanna et al. [12] Trained machine and deep learning models based on tissue characterization for assessing cardiovascular risk in RA patients and explored the impact of RA on CVD risk levels with a focus on bone sensitivity and surface classification.

Cao et al. [13] Used image analysis for segmenting 3-D bone surfaces and joints, achieving an impressive accuracy of 0.97. This study highlights the potential of advanced imaging techniques in accurately delineating bone structures in the context of RA.

Qazi et al. [14] proposed an auto-segmentation method on head and neck CT images, contributing to the broader field of automated segmentation in medical imaging. Although not specific to RA, the methodology addresses the challenges of automated segmentation in diverse medical imaging contexts.

Manzke et al. [15] Explored the automatic segmentation of rotational X-ray images for generating intra-procedural surface models in atrial fibrillation ablation procedures. The study showcases potential applications of automated segmentation in various medical procedures.

Finckh et al. [16] evaluated the performance of an automated computer-based scoring method for assessing joint space narrowing in RA. This longitudinal study provides a quantitative measure for tracking disease progression with an accuracy of 0.95.

Ichikawa et al. [17] employed a computer-based approach using temporal subtraction in rheumatoid wrist radiographs to quantify joint space narrowing progression and focused on enhancing the accuracy of radiographic quantifications through innovative image processing techniques.

Khan et al. [18] discussed the burden of non-communicable diseases, including RA, in transition communities. While not directly related to imaging, this epidemiological study highlights the broader impact of RA on public health in urban and rural regions.

Wang et al. [19] provided a comprehensive survey of artificial intelligence applications in RA, they covered image-based diagnosis, predictive modeling, and the integration of AI into routine clinical practice.

Avramidis et al. [20] Compared rheumatoid arthritis diagnosis using deep learning versus traditional human-based methods. They Contributed valuable insights into the potential role of artificial intelligence in improving diagnostic accuracy and efficiency.

Wang et al. [21] Proposed a deep learning-based computer-aided diagnosis system for RA using hand X-ray images and aiming to enhance the objectivity and precision of RA diagnosis through advanced image analysis techniques.

Wu et al. [22] Presented a deep-learning classification of metacarpophalangeal joints synovial proliferation in RA using ultrasound images. The research focuses on leveraging advanced computational methods for the automated assessment of synovial involvement in RA.

3. Methodology

We Introduced an innovative method for diagnosing the stages of Rheumatoid Arthritis (RA). We initially employed augmentation with a R-GAN to augment the dataset and integrate genuine and synthetic samples. Subsequently, a Convolutional Neural Network (CNN) model was trained using this augmented dataset. Figure 1 illustrates the complete proposed model.

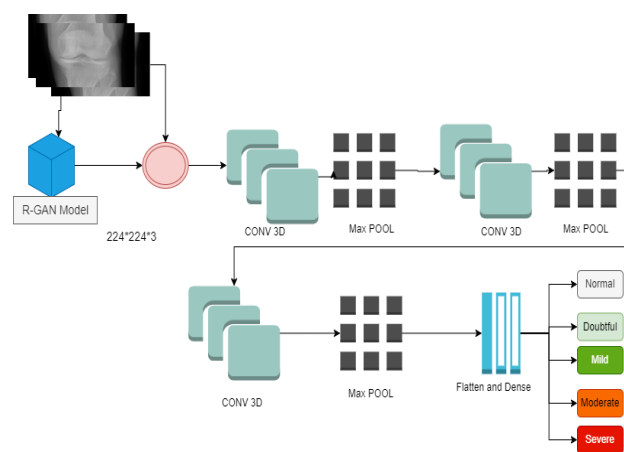


Fig 1 architecture of proposed system

3.1 Dataset and Augmentation

In this methodology, the Kaggle Knee dataset [25] was employed, and it was observed that the original dataset contained a limited number of samples, as indicated in Table 1. To address this limitation, we applied the Regularized Generative Adversarial Network (R-GAN) to generate artificial samples to balance the

sample distribution across all classes. Ultimately, this augmentation process generated a total of 5000 samples for each class, and the total number of samples after balancing is 7310.

	Normal	Doubtful	Mild	Moderate	Severe	Total
Actual number of samples	514	477	232	221	206	1650
Augmented samples	514	514	514	514	514	2570
Actual and R-GAN Samples	1462	1462	1462	1462	1462	7310

In the R-GAN implementation, the discriminator and generator's loss parameters were fine-tuned to a specific threshold value set at 1. This adjustment in the loss threshold aimed to optimize the training dynamics of the R-GAN model and enhance its performance in generating synthetic samples while maintaining stability in the adversarial training process. Loss of Discriminator is $L_D = Error(D(x), 1) + Error(D(G(x)), 0)$ and loss function for Generator is $L_G = Error(D(G(x)), 1)$ from this with cross entropy loss function we optimized the both the losses with respect to N_{sp} .

$$\frac{p_{data}(x)}{D(x)} = N_{sp} + \frac{p_g(x)}{1-D(x)} \quad (1)$$

$$\frac{p_{data}(x)}{D(x)} = \frac{N_{sp} - N_{sp} D(x) + p_g(x)}{1-D(x)} \quad (2)$$

$$D(x) = \frac{(1-D(x))p_{data}(x)}{N_{sp} - N_{sp} D(x) + p_g(x)} \quad (3)$$

$$V(G, D) = E_{x-p_{data}} [\log(D(x))] + E_{x-p_g} [\log(1 - D(x))] \quad (4)$$

$$V(G, D) = E_{x-p_{data}} \left[\log \left(\frac{(1-D(x))p_{data}(x)}{N_{sp} - N_{sp} D(x) + p_g(x)} \right) \right] + E_{x-p_g} \left[\log \left(1 - \frac{1-D(x)p_{data}(x)}{N_{sp} - N_{sp} D(x) + p_g(x)} \right) \right] \quad (5)$$

Where N_{sp} is the noised data, range between $0 < N_{sp} \leq 1$. Equation (5) is the derived optimizer for R-GAN. And x is the real data, $G(x)$ synthetic data, $D(x)$ discriminator evaluation for real data, and $D(G(x))$ is generator evaluation for synthetic data, fig 2 illustrates sample which is generated with GAN.

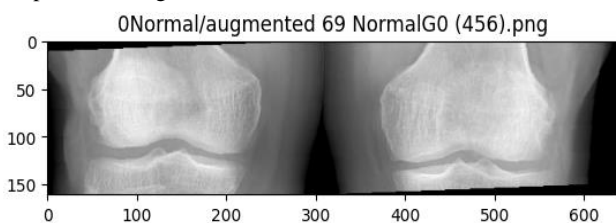


Fig 2 augmented sample with GAN

3.2 Implementation

As depicted in Figure 1, we implemented an optimized CNN model comprising three convolutional layers and three max-pooling layers. Subsequently, the array was flattened into a single dimension and mapped to the output layer. Post-augmentation, the dataset consisted of 7310 samples distributed across five classes. All samples were resized to dimensions of 224x224, and the dataset was partitioned into training, testing, and validation sets in a ratio of 75:15:10. Throughout 35 epochs, the model underwent training with variations in parameters, including different batch sizes. Results were closely monitored to identify potential overfitting or underfitting issues. A fixed learning rate of 0.001 was maintained during each iteration to ensure consistency in the training process.

4. Result Analysis

The model underwent training with various batch sizes in our experimentation, including 8, 16, and 32, each for 35 epochs. Throughout this process, we closely monitored the accuracy and consistency of the model's performance. Notably, the model exhibited exceptional accuracy at a batch size of 16, achieving a noteworthy 0.97. This high accuracy was consistent across training and validation sets, as evidenced by the observed training and validation loss and accuracy trends.

Figure 3 visually represents the confusion matrix on the test data. The analysis reveals a high true-positive rate and a notable false-negative rate, indicating the model's proficiency in correctly identifying positive instances and suggesting areas for potential improvement, particularly in reducing false negatives.

Moreover, Figure 4 depicts the training and validation loss and the accuracy over the training epochs. The consistent downward trend in training and validation loss signifies effective learning and model convergence. Simultaneously, the consistent increase in accuracy across epochs further substantiates the model's reliability. Interestingly, our observation from Figure 4 indicates that the 14th epoch is optimal. The model balances low loss and high accuracy during this epoch, demonstrating its peak performance. This insight into the optimal epoch can guide future training strategies and improve the model's efficiency.

		Confusion Matrix				
		0Normal	1Doubtful	2Mild	3Moderate	4Severe
Actual	0Normal	120	0	0	1	0
	1Doubtful	1	119	0	1	0
	2Mild	0	0	120	1	0
	3Moderate	0	0	0	121	0
	4Severe	0	0	0	0	121
		0Normal	1Doubtful	2Mild	3Moderate	4Severe
		Predicted				

Fig 3 Confusion matrix of proposed model

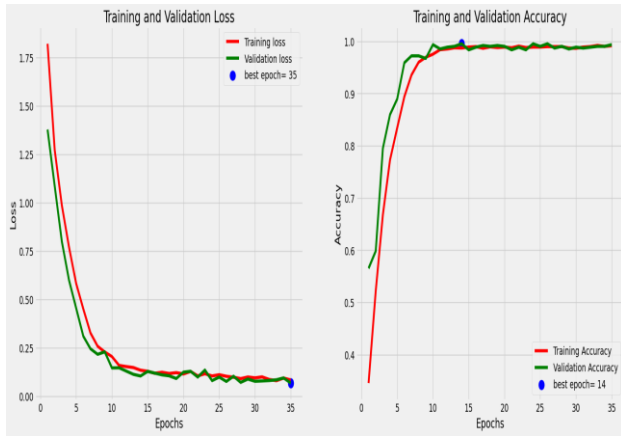


Fig 4. Training and validation loss and accuracy

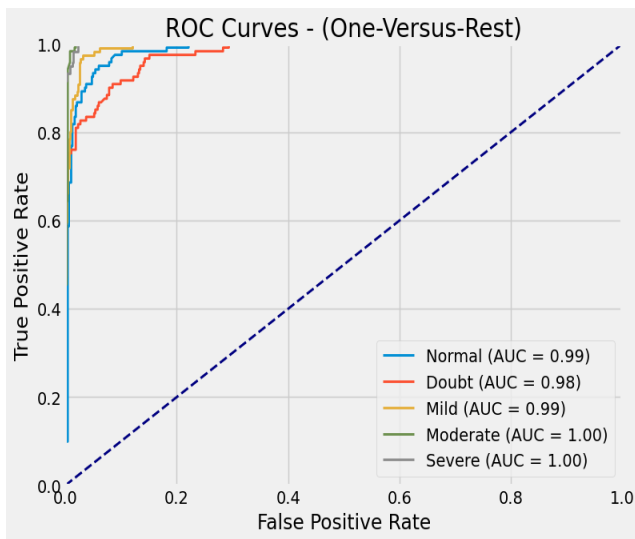


Fig 5 ROC curve of proposed model over all classes

The ROC curve analysis, presented in Figure 5 for each class, provides compelling evidence of the model's excellent accuracy, with AUC values ranging from 0.98 to 1. These high AUC values signify robust performance, distinguishing between true positive and false positive rates across different classes.

The detailed evaluation metrics in Table 2 further reinforce the model's reliability. Precision, recall, and F1-score results consistently demonstrate strong performance across all classes, with a substantial support count of 121. The support count, indicating the number of instances for each class, underscores the model's proficiency in handling a substantial dataset.

The final accuracy of 0.97 is noteworthy, reflecting the model's overall effectiveness in accurately classifying knee X-ray images. The combination of high AUC values, consistent precision, recall, and F1-score results, along with a substantial support count, contributes to the comprehensive validation of the model's robustness.

Additionally, Table 3 provides a comparative analysis between our proposed and existing models. The results indicate that our model performed exceptionally well, outperforming several existing models. Notably, Model [8] achieved similar performance, but it is worth highlighting that some of these models classified the problem into two classes, distinguishing between RA and non-RA. In contrast, our model, handling the task across multiple classes, demonstrates its versatility and effectiveness in a more nuanced classification scenario.

	Precision	recall	F1-score	Support
0	0.971	0.99	0.981	121
1	0.95	0.95	0.951	121
2	0.955	0.971	0.97	121
3	0.972	0.971	0.98	121
4	0.98	0.981	0.99	121
Accuracy			0.97	605
Macro avg	0.97	0.97	0.97	605
Weighted Avg	0.97	0.97	0.97	605

Table 2 R-GAN net model results with simple CNN model for tuned hyper parameters

System	Model Implemented	Number classes	Accuracy
[6]	SVM		0.91
[8]	RANet, QNN	2	0.95, 0.97
[10]	6 machine learning models	5	0.85
[11]	SVM	5	0.85
Proposed Model with Annotation of samples	CNN	5	0.95
Proposed Model with Augmenting samples	RCNN	5	0.97

Table 3. Comparison of proposed model with existing model

5. Conclusion

This paper presents a comprehensive knee X-ray image classification approach that has yielded a highly effective model. Our methodology involves initial data augmentation using R-GAN, generating synthetic samples with a loss of 0.1. This augmentation process successfully addresses class imbalance concerns, initially present in the actual set of 1650 samples. The final dataset, totaling 7,310 samples, trains our optimized CNN model. The CNN model is fine-tuned by carefully exploring hyperparameters, showcasing impressive performance trends over 35 epochs.

The ROC curve analysis emphasizes the model's superior true favorable rates, particularly in the balanced dataset, affirming its discriminative capabilities with an accuracy of 0.97.

Furthermore, we compared our model's accuracy against all existing models, revealing that our approach outperformed other models in the context of knee X-ray image classification. This observation underscores the effectiveness and superiority of our proposed methodology.

Author contributions

Saloni Fathima: Conceptualization, Methodology, Software, Field study, Validation., Field study, Visualization,

Shankar Lingam G: Data curation, Writing-Original draft preparation, Software, Investigation, Writing-Reviewing and Editing.

Conflicts of interest

The authors declare no conflicts of interest.

References

- [1] Snehalatha U, Rajalakshmi T, Gopikrishnan M, Gupta N. Computer-based automated analysis of X-ray and thermal imaging of knee region in evaluation of rheumatoid arthritis. *Proc Inst Mech Eng H*. 2017 Dec;231(12):1178-1187. Doi: 10.1177/0954411917737329. Epub 2017 Oct 27. PMID: 29076764.
- [2] Snehalatha U, Anburajan M, Sowmiya V, Venkatraman B, Menaka M. Automated hand thermal image segmentation and feature extraction in the evaluation of rheumatoid arthritis. *Proc Inst Mech Eng H*. 2015 Apr;229(4):319-31. Doi: 10.1177/0954411915580809. PMID: 25934260.
- [3] Snehalatha U, Anburajan M. Computer-based measurements of joint space analysis using metacarpal morphometry in hand radiograph for evaluation of rheumatoid arthritis. *Int J Rheum Dis*. 2017 Sep;20(9):1120-1131. Doi: 10.1111/1756-185X.12559. Epub 2015 Apr 10. PMID: 25865479.
- [4] Snehalatha U, Muthubhairavi V, Anburajan M, Gupta N. Ultrasound Color Doppler Image Segmentation and Feature Extraction in MCP and Wrist Region in Evaluation of Rheumatoid Arthritis. *J Med Syst*. 2016 Sep;40(9):197. Doi: 10.1007/s10916-016-0552-z. Epub 2016 Jul 23. PMID: 27449351.
- [5] Parashar A, Rishi R, Parashar A, Rida I. Medical imaging in rheumatoid arthritis: A review on deep learning approach. *Open Life Sci*. 2023 Jul 6;18(1):20220611. Doi: 10.1515/biol-2022-0611. PMID: 37426615; PMCID: PMC10329279.
- [6] Bardhan S, Bhowmik MK. 2-Stage classification of knee joint thermograms for rheumatoid arthritis prediction in subclinical inflammation. *Australas Phys Eng Sci Med*. 2019 Mar;42(1):259-277. doi: 10.1007/s13246-019-00726-9. Epub 2019 Jan 31. PMID: 30706334.
- [7] Hemalatha RJ, Vijaybaskar V, Thamizhvani TR. Automatic localization of anatomical regions in medical ultrasound images of rheumatoid arthritis using deep learning. *Proc Inst Mech Eng H*. 2019 Jun;233(6):657-667. doi: 10.1177/0954411919845747. Epub 2019 Apr 24. PMID: 31017534.
- [8] Ahalya RK, Almutairi FM, Snehalatha U, Dhanraj V, Aslam SM. RANet: a custom CNN model and convolutional neural network for the automated detection of rheumatoid arthritis in hand thermal images. *Sci Rep*. 2023 Sep 20;13(1):15638. Doi: 10.1038/s41598-023-42111-3. PMID: 37730717; PMCID: PMC10511741.
- [9] Srinivasan S, Gunasekaran S, Mathivanan SK, Jayagopal P, Khan MA, Alasiry A, Marzougui M, Masood A. "A Framework of Faster CRNN and VGG16-Enhanced Region Proposal Network for Detection and Grade Classification of Knee RA. *Diagnostics (Basel)*". 2023 Apr 10;13(8):1385. Doi: 10.3390/diagnostics13081385. PMID: 37189485; PMCID: PMC10137623.
- [10] Xiao J, Wang R, Cai X, Ye Z. "Coupling of Co-expression Network Analysis and Machine Learning Validation Unearthed Potential Key Genes Involved in Rheumatoid Arthritis. *Front Genet*". 2021 Feb 11;12:604714. Doi: 10.3389/fgene.2021.604714. PMID: 33643380; PMCID: PMC7905311.
- [11] Chen Y, Liao R, Yao Y, Wang Q, Fu L. "Machine learning to identify immune-related biomarkers of rheumatoid arthritis based on WGCNA network. *Clin Rheumatol*". 2022 Apr;41(4):1057-1068. Doi: 10.1007/s10067-021-05960-9. Epub 2021 Nov 12. PMID: 34767108.
- [12] Khanna NN, Jamthikar AD, Gupta D, Piga M, Saba L, Carcassi C, Giannopoulos AA, Nicolaides A, Laird JR, Suri HS, Mavrogeni S, Protogerou AD, Sfrikakis P, Kitas GD, Suri JS. "Rheumatoid Arthritis: Atherosclerosis Imaging and Cardiovascular Risk Assessment Using Machine and Deep Learning-Based Tissue Characterization. *Curr Atheroscler Rep*". 2019 Jan 25;21(2):7. Doi: 10.1007/s11883-019-0766-x. PMID: 30684090.
- [13] Cao K, Mills DM, Thiele RG, Patwardhan KA. "Toward Quantitative Assessment of Rheumatoid Arthritis Using Volumetric Ultrasound". *IEEE Trans Biomed Eng*. 2016 Feb;63(2):449-58. doi: 10.1109/TBME.2015.2463711. Epub 2015 Aug 4. PMID: 26258932.
- [14] Qazi AA, Pekar V, Kim J, Xie J, Breen SL, Jaffray DA. "Auto-segmentation of normal and target structures in head and neck CT images: a feature-driven model-based approach". *Med Phys*. 2011 Nov;38(11):6160-70. doi: 10.1118/1.3654160. PMID: 22047381.
- [15] Manzke R, Meyer C, Ecabert O, Peters J, Noordhoek NJ, Thiagalingam A, Reddy VY, Chan RC, Weese J. "Automatic segmentation of rotational x-ray images for anatomic intra-procedural surface generation in atrial fibrillation ablation procedures". *IEEE Trans Med Imaging*. 2010 Feb;29(2):260-72. doi: 10.1109/TMI.2009.2021946. PMID: 20129843.
- [16] Finckh A, de Pablo P, Katz JN, Neumann G, Lu Y, Wolfe F, Duryea J. "Performance of an automated computer-based scoring method to assess joint space narrowing in rheumatoid arthritis: a longitudinal study. *Arthritis Rheum*". 2006 May;54(5):1444-50. doi: 10.1002/art.21802. PMID: 16645974.
- [17] Ichikawa S, Kamishima T, Sutherland K, Okubo T, Katayama K. "Radiographic quantifications of joint space narrowing progression by computer-based approach using temporal subtraction in rheumatoid wrist". *Br J Radiol*. 2016;89(1057):20150403. doi: 10.1259/bjr.20150403. Epub 2015 Oct 20. PMID: 26481695; PMCID: PMC4985954.
- [18] Khan, F. S., Lotia-Farrukh, I., Khan, A. J., Siddiqui, S. T., Sajun, S. Z., Malik, A. A., ... & Fisher-Hoch, S. P. (2013). The burden of non-communicable disease in transition communities in an Asian megacity: baseline findings from a cohort study in Karachi, Pakistan. *PLoS one*, 8(2), e56008.
- [19] Wang J, Tian Y, Zhou T, Tong D, Ma J, Li J. A survey of artificial intelligence in rheumatoid arthritis. *Rheumatol Immunol Res*. 2023 Jul 22;4(2):69-77. doi: 10.2478/rir-2023-0011. PMID: 37485476; PMCID: PMC10362600.
- [20] Avramidis, G. P., Avramidou, M. P., & Papakostas, G. A. (2021). Rheumatoid arthritis diagnosis: Deep learning vs. humane. *Applied Sciences*, 12(1), 10.
- [21] Wang, H. J., Su, C. P., Lai, C. C., Chen, W. R., Chen, C., Ho, L. Y., ... & Lien, C. Y. (2022). Deep learning-based Computer-Aided diagnosis of rheumatoid arthritis with hand X-ray images Conforming to Modified total Sharp/van der Heijde score. *Biomedicines*, 10(6), 1355.
- [22] Wu, M., Wu, H., Wu, L., Cui, C., Shi, S., Xu, J., ... & Dong, F. (2022). A deep learning classification of metacarpophalangeal joints synovial proliferation in rheumatoid arthritis by ultrasound images. *Journal of Clinical Ultrasound*, 50(2), 296-301.
- [23] Salaffi, F., Sarzi-Puttini, P., Girolimetti, R., Atzeni, F., Gasparini, S., & Grassi, W. (2009). Health-related quality of life in fibromyalgia patients: a comparison with rheumatoid arthritis patients and the general population using the SF-36 health survey. *Clinical & Experimental Rheumatology*, 27(5), S67.
- [24] Sayah, A., & English III, J. C. (2005). Rheumatoid arthritis: a review of the cutaneous manifestations. *Journal of the American Academy of Dermatology*, 53(2), 191-209.
- [25] Gornale, Prof. Shivanand; Patravali, Pooja (2020), "Digital Knee X-ray Images", *Mendeley Data*, V1, doi: 10.17632/t9ndx37v5h.1